A ^{29}Si MAS NMR study of silicate glasses with a high lithium content

2006 J. Phys.: Condens. Matter 18 11323

(http://iopscience.iop.org/0953-8984/18/49/023)

INSTITUTE OF PHYSICS PUBLISHING JOURNAL OF PHYSICS: CONDENSED MATTER

J. Phys.: Condens. Matter **18** (2006) 11323–11331 doi:10.1088/0953-8984/18/49/023

A ^{29}Si MAS NMR study of silicate glasses with a high lithium content

C Larson[1], J Doerr[1], M Affatigato[1], S Feller[1], D Holland[2] and M E Smith[2]

[1] Physics Department, Coe College, Cedar Rapids, IA 52402, USA
[2] Department of Physics, University of Warwick, Coventry CV4 7AL, UK

Received 3 July 2006, in final form 31 October 2006
Published 23 November 2006
Online at stacks.iop.org/JPhysCM/18/11323

Abstract

A series of lithium silicate glasses approaching the orthosilicate composition (66.7 mol% Li_2O) were prepared and their ^{29}Si magic angle spinning nuclear magnetic resonance (NMR) recorded; this significantly extends the compositional range of glasses studied by this technique. The results indicate that the lever (binary) rule is approximately followed, though with considerable dissociation of the stoichiometric groups into silicate units with lesser and greater numbers of non-bridging oxygens according to the relation $2Q^n \rightarrow Q^{n+1} + Q^{n-1}$. The NMR results were compared with the Raman study of Umesaki *et al* (1988 *J. Non-Cryst. Solids* **106** 77–80) on the same system. Volumes per mol silica, determined from the experimental densities, were also used to test the structural results from the present NMR observations.

(Some figures in this article are in colour only in the electronic version)

1. Introduction

The standard structural model for alkali silicate glasses indicates that alkali oxide enters the silicate network in such a way as to convert bridging oxygens to non-bridging oxygens whilst maintaining silica tetrahedra. The result is a glass with a mixture of Q^n tetrahedra where n represents the number of bridging oxygens per silicon and may take values of 0 to 4 in integer steps. Solid state magic angle spinning (MAS) nuclear magnetic resonance (NMR) has been widely used to provide information on the local environment of silicon in glass [1]. Dupree *et al* and Maekawa *et al* demonstrated [2, 3] through the use of ^{29}Si MAS NMR, that this structural view continues quantitatively from about 25 to 40 mol% Li_2O, with glass formation limited by phase separation on the low alkali side and by crystallization on the high alkali side.

We report NMR results for glasses, produced using rapid cooling, that increase the range of known data up to 64.3 mol% Li_2O. Glass formation, even using roller quenching for maximal cooling rates, ceases past this composition. This limit is presumably due to the end of a covalent network, as indicated by the present results, and which may be predicted on the basis of composition to happen when the short-range structural units in the material

Table 1. Fit parameters for ^{29}Si NMR spectra of the lithium silicate glasses. ΔQ^n is the width and δQ^n is the chemical shift of the fitted peak from the Q^n silicate group referenced to TMS. The error in both δQ^n and ΔQ^n is 0.5 ppm.

x	$J = x/(1-x)$	δQ^4	ΔQ^4	δQ^3	ΔQ^3	δQ^2	ΔQ^2	δQ^1	ΔQ^1	δQ^0	ΔQ^0
0.375	0.6	−99.0	14.9	−87.0	13.2	−78.3	7.9	−70.7	7.6		
0.444	0.8			−87.0	12.9	−78.4	9.1	−69.0	5.9		
0.500	1.0			−86.0	11.0	−78.0	8.7	−70.7	5.9		
0.545	1.2			−86.0	11.0	−76.1	9.5	−70.0	7.1		
0.583	1.4					−76.0	10.0	−70.5	6.1	−65.1	6.3
0.615	1.6					−74.6	8.0	−69.8	6.1	−64.9	4.9
0.643	1.8					−75.7	6.7	−70.5	5.4	−65.4	4.7

are fully depolymerized, i.e. when all silica tetrahedra are solely Q^0 ($[SiO_4]^{4-}$) groups at 66.7 mol% Li_2O. It could be argued that the network should cease to exist earlier than this, when the glass contains predominantly isolated pyrosilicate groups ($[Si_2O_7]^{6-}$ containing Q^1 silicons). Stoichiometrically, this would occur at 60 mol% Li_2O. The fact that glasses can be made beyond this composition suggests that there is a distribution of Q^n types present, which contribute sufficient structural confusion such that crystallization can be prevented by a sufficiently high cooling rate.

2. Experimental procedures

2.1. Glass formation

The glasses were made from silica (reagent grade or better from Aldrich Inc.) and lithium carbonate (reagent grade or better from Aldrich Inc.). Appropriate amounts of the batch compounds were thoroughly mixed in a platinum crucible and the resulting mixture was heated in the range 1300–1400 °C until a clear, colourless melt was produced (after about 20 min). The samples were cooled, weighed, reheated for several minutes, and subsequently quenched either by quenching the crucible in an ice-water bath (only for the sample with 37.5 mol% Li_2O) or through the use of a roller-quencher [4], producing a cooling rate of about 10^5 K s^{-1}. The roller-quencher consists of two 15 cm stainless steel rollers with a gap of about 25 μm and a rotation rate of several hundred rpm. Weight loss measurements of the samples confirm the full removal of carbon dioxide and the completion of the chemical reaction (1):

$$x\mathrm{Li_2CO_3} + (1-x)\mathrm{SiO_2} \rightarrow x\mathrm{Li_2O}\cdot(1-x)\mathrm{SiO_2} + x\mathrm{CO_2}. \quad (1)$$

Table 1 lists the batch compositions of the resulting samples. In this table and throughout the paper composition is also given by J, the molar ratio of alkali oxide to silica or

$$J = x/(1-x). \quad (2)$$

J is used instead of mole fraction for convenience in linearizing the structural model and simplifying the graphical presentations.

2.2. Nuclear magnetic resonance

^{29}Si MAS NMR was performed on the samples at 8.45 T on a CMX360 spectrometer using a Chemagnetics 6 mm probe and rotating the sample at ∼5.8 kHz at the magic angle. The silicon spectra were obtained at 71.54 MHz, with a pulse length of 1.2 μs($\sim\pi/6$) and a pulse delay of

Table 2. Percentages of the Q^n groups in lithium silicate glasses from the present work.

x (mol % Li_2O)	J $(x/(1-x))$	J (from fit)	Per cent of Q^4	Per cent of Q^3	Per cent of Q^2	Per cent of Q^1	Per cent of Q^0
0.375	0.60	0.66 (±0.06)	6 (±3)	59 (±3)	32 (±3)	3 (±3)	0
0.444	0.80	0.79 (±0.06)	0	45 (±3)	52 (±3)	3 (±3)	0
0.500	1.00	1.00 (±0.06)	0	19 (±3)	64 (±3)	18 (±3)	0
0.545	1.20	1.18 (±0.06)	0	6 (±3)	53 (±3)	41 (±3)	0
0.583	1.40	1.41 (±0.08)	0	0	35 (±3)	48 (±3)	17 (±3)
0.615	1.60	1.63 (±0.08)	0	0	8 (±3)	63 (±3)	30 (±3)
0.643	1.80	1.79 (±0.08)	0	0	3 (±3)	33 (±3)	63 (±3)

120 s. This delay was found to be sufficient to ensure relaxation, and hence quantitative spectra, in spite of the absence of paramagnetic additions. Typically 500–600 scans were acquired and a line broadening of 50 Hz applied prior to Fourier transformation. Tetramethylsilane (TMS) was used as the primary reference at 0 ppm.

3. Results

Figure 1 presents the resulting ^{29}Si MAS NMR spectra for the seven glasses studied. The main peaks are shown for clarity but the spinning sidebands were included in the peak fitting process. Gaussian lineshapes were used to fit the contributions from Q^4, Q^3 and Q^2. However, the peaks from Q^1 and Q^0 were significantly narrower and further it was found that a better fit was obtained using a pseudo-Voigt function with a 66% Lorentzian contribution. At a spinning speed of 5.8 kHz, the sidebands are sufficiently far removed from the main peaks that they only represent ∼4–5% of the total intensity. Generally, only the sidebands from the most intense peaks could be fitted. Failure to fit sideband intensity from all of the peaks is estimated to result in an error of ∼0.5% on the intensity of a given Q^n contribution. Sidebands were not observed for the symmetric Q^4 and Q^0 species, as expected. Some representative peak fits are given in figure 2. Table 1 lists the parameters found from the fitting. The widths (defined by ΔQ^n) and the peak positions (defined by δQ^n) of the $J = 0.6$ glass were compared to those found by Dupree *et al* [2] and Maekawa *et al* [3] as this sample is in the range of the reported compositions in these studies. The peak positions of the Q^n species reported by Maekawa are about 3 ppm lower for Q^4 and 3 ppm higher each for Q^2 and Q^1, respectively. The widths of the peaks associated with each Q^n unit also vary somewhat, Maekawa's ΔQ^4 being approximately 3 ppm wider, ΔQ^3 about 4 ppm narrower and ΔQ^2 about 0.5 ppm narrower. The fitting results from Dupree *et al* [2] are in excellent accord with the present results. The peak positions found by Dupree *et al* differ by just 1 to 2 ppm whereas the peak widths are within 1 ppm. The resulting fractions of the Q^n units are presented in table 2 and figure 3. The fits also provide an independent check on composition from the following relationship:

$$100\ J\ (\text{from fit}) = Q^4(0) + Q^3(0.5) + Q^2(1) + Q^1(1.5) + Q^0(2). \tag{3}$$

The results of this calculation agree within experimental error with batch compositions (see table 2). Figure 3 also presents the Q^n fractions superposed on the idealized lever rule

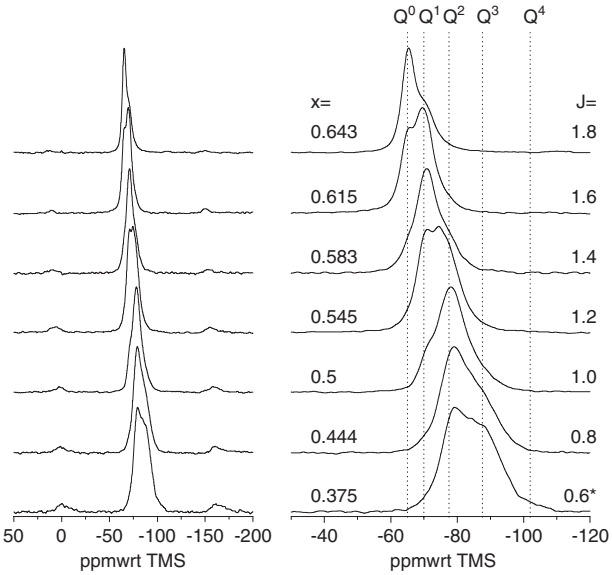

Figure 1. ^{29}Si MAS NMR spectra from lithium silicate glasses prepared for this study. J is the molar ratio of lithia to silica and x is the molar fraction of lithia. $*$ the $J = 0.6$ sample was prepared by conventional quenching. The right-hand sequence shows expanded plots of the central peaks and the left-hand sequence also shows the spinning sidebands.

model along with data from Dupree *et al* [2] and Maekawa *et al* [3] at relatively low alkali concentrations.

4. Discussion

The simplest model for the structure of lithium silicate glasses is the lever or binary rule. As the silicate glass is modified by lithia this model assumes sequential conversion of the silica tetrahedra:

$$Q^n \rightarrow Q^{n-1}. \tag{4}$$

The conversions between the Q_n units using the lever rule [3, 5] may be written fractionally as linear relationships in terms of J, the molar ratio of Li_2O to SiO_2:

$$Q^4 = 1 - 2J, \qquad Q^3 = 2J \qquad 0.0 \leqslant J \leqslant 0.5 \tag{5a}$$

$$Q^3 = 2 - 2J, \qquad Q^2 = 2J - 1 \qquad 0.5 \leqslant J \leqslant 1.0 \tag{5b}$$

$$Q^2 = 3 - 2J, \qquad Q^1 = 2J - 2 \qquad 1.0 \leqslant J \leqslant 1.5 \tag{5c}$$

$$Q^1 = 4 - 2J, \qquad Q^0 = 2J - 3 \qquad 1.5 \leqslant J \leqslant 2.0. \tag{5d}$$

Plots of the lever rule as a function of J also are found in figure 3.

The present data are in reasonable agreement with the earlier results from Dupree *et al* [2] and Maekawa *et al* [3] where the two data sets have similar low alkali concentrations (figure 3). In the former work samples were formed by quenching the melt between two metal plates [2], whilst in the latter the samples were quenched in water or liquid nitrogen [3]. Further, it is clear from an examination of figure 3 that there is a systematic evolution of the Q^n units from Q^n to Q^{n-1}, but with considerable disproportionation present as well:

$$2Q^n \rightarrow Q^{n+1} + Q^{n-1}. \tag{6}$$

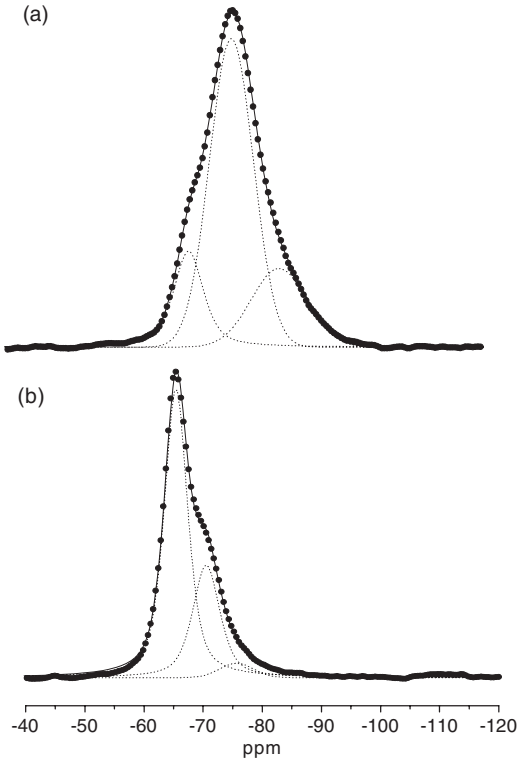

Figure 2. Peak fitting for the (a) $J = 1.0$ and (b) $J = 1.8$ lithium silicate glasses. J is the molar ratio of lithia to silica.

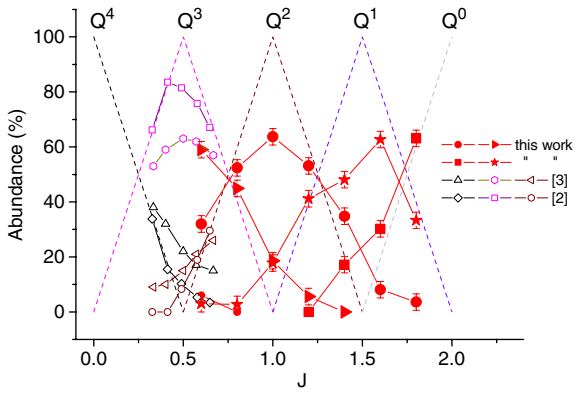

Figure 3. Fractions of the Q^n groups in lithium silicate glasses as a function of J, the molar ratio of lithia to silica. Data are from Dupree *et al* [2] (open squares and open diamonds), Maekawa *et al* [3] (open circles and open triangles) and the present work (solid symbols). Dotted lines are the idealized lever rule.

Rather than following the idealized lever (binary) rule model the data are generally between this model and a purely statistical model for the Q^n units [6]. For example, in the case of a glass with 50 mol% Li_2O, the lever rule predicts that 100% of the silica tetrahedra

Table 3. D, deviation of main Q^n species from the lever rule for lithium silicate glasses.

J	Main Q^n species present	D, the deviation of the main Q^n species from the lever rule $= (Q^{\text{ncalc}} - Q^{\text{nexp}})/Q^{\text{ncalc}}$
0.6	Q^3	0.26
0.8	Q^2	0.12
1.0	Q^2	0.36
1.2	Q^2	0.12
1.4	Q^1	0.40
1.6	Q^1	0.22
1.8	Q^0	0.22

Table 4. Equilibrium constants, K_n, for the Q^n species in lithium silicate glasses.

J	K_n	$K_n = [Q^{n+1}][Q^{n-1}]/([Q^n])^2$
0.6	K_3	0.055 ($[Q^1]$ ignored)
0.8	K_2	0.044
1.0	K_2	0.082
1.2	K_2	0.088
1.4	K_1	0.258
1.6	K_1	0.062
1.8	K_0	—

should be Q^2 but the NMR results show that only about 60% of the glass is composed of silicons in Q^2 groups with about 20% of the silicons in Q^3 and 20% in Q^1 configurations. In a purely statistical distribution of the Q^n units, about 38% of the silicons would be Q^2, 25% Q^1 and Q^3 each, and 6% Q^4 and Q^0 each [6]. It has been known [2, 3] for some time that the disproportionation is greater in lithium when compared to the sodium and potassium systems, when measured at low alkali contents. As J increases towards the orthosilicate ($J = 2$) composition the two models approach both each other and also the data, since the structure should then be entirely composed of Q^0 units.

Another indication of the amount of disproportionation is found by determining the average difference between lever rule values (Q^{ncalc}) and fitted values of the main species present at any given composition (Q^{nexp}). The deviation, D, is expressed by

$$D = (Q^{\text{ncalc}} - Q^{\text{nexp}})/Q^{\text{ncalc}}. \tag{7}$$

The results of this calculation are displayed in table 3. The amount of disproportionation is maximal at or near a stoichiometric composition for one of the Q^n units, with the exception of the Q^0 unit. The Q^0 unit cannot disproportionate as J approaches 2 since it is the silicate with the highest lithium content, being saturated with non-bridging oxygens.

Equilibrium constants, K_n, were also determined using the concentrations of the Q^n species:

$$K_n = [Q^{n+1}][Q^{n-1}]/([Q^n])^2. \tag{8}$$

The resulting K_n values are given in table 4. The system is of course far from equilibrium and these values are controlled by the equilibrium in the melt, the effectiveness of the cooling and the change of viscosity with temperature.

The present structural results are also manifested in a plot of the volume per mol SiO_2 [7, 8] versus composition. These data are plotted as a function of J in figure 4, and include high

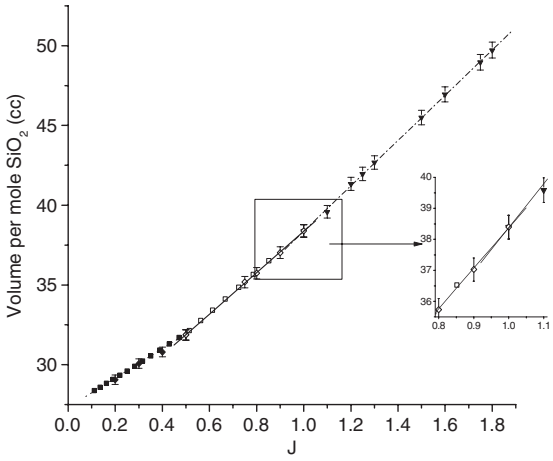

Figure 4. Volume per mol SiO_2 as a function of J, the molar ratio of lithium oxide to silicon dioxide. Data from Bansal and Doremus [8] are shown larger than the error bars (solid and open squares). All symbols with error bars represent data from Peters *et al* [7].

lithia-content glasses of similar composition to those reported here [7]. These volumes change linearly as J increases and the linearity is indicative of simple Q^n unit changes; or in other words as a Q^{n+1} unit is formed from a Q^n group by the addition of half an oxygen and a lithium ion the volume per silicon increases at a uniform rate. The slope of these volumes increase as J increases in steps of 0.5 (because the Q^n units are separated from the Q^{n+1} in composition by $J = 0.5$) and this change in slope is indicative of the silicate unit changes as Q^n units acquire more volume as more non-bridging oxygens are formed at the expense of bridging oxygens.

In the ideal lever (binary) model Q^3 and Q^2 each have an abundance of 100% at $J = 0.5$ and 1.0, respectively. Below $J = 0.5$ there will be an admixture of Q^4 and Q^3 whereas for $0.5 \leqslant J \leqslant 1.0$ there will be a linear combination of the Q^3 and Q^2 units. This structural view is supported by the slope change seen in figure 4. A similar change in slope occurs at $J = 1$, although it is less pronounced than in the lower J case. The smaller increase in slope for the higher J transition past $J = 1$ may be understood, to first order, in terms of the fractional volume changes per silicon in terms of oxygen number since oxygen is the largest ion by a considerable margin. Below $J = 0.5$ the oxygen increase per silicon is 0.5 on a base of 2 ($Q^4 \rightarrow Q^3$), whereas past $J = 0.5$ it is an increase of 0.5 on a base of 2.5 ($Q^3 \rightarrow Q^2$). This compares to the transition at $J = 1$ where below $J = 1$ the change is 0.5 on a base of 2.5 and past $J = 1$ it is 0.5 on a base of 3.0 ($Q^2 \rightarrow Q^1$). Thus, the volume change per silicon is less pronounced for the $J = 1$ transition when compared to the $J = 0.5$ transition.

However, as indicated, the NMR data indicate the presence of some disproportionation. The comparison of the volumes per silicon with the NMR data implies that the density is really reflecting an average coordination change in the Q_n units; evidently this is still enough to cause uniform and distinctive changes in density and volume trends.

In addition, the present results are in reasonable agreement with a Raman study of high lithia content glass performed by Umesaki *et al* [9]. Figure 5 displays a comparison of the abundances of the Q^n units obtained from the present NMR results with those found from the Raman study on glasses also prepared by roller quenching [8]. The agreement is good, especially given the fact that the Raman spectra were deconvoluted and the resulting intensities

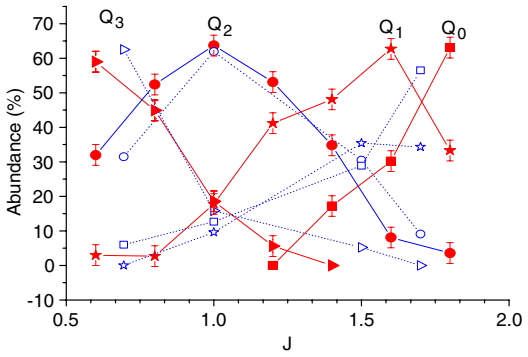

Figure 5. Comparison of the Q^n unit abundances from the present ^{29}Si MAS NMR data (solid symbols) and the Raman results (open symbols) from Umesaki *et al* [9]. The data are plotted as a function of J, the molar ratio of lithium oxide to silicon dioxide.

related to the structural abundances assuming that each Q^n site had the same Raman cross section, although the normalized Raman relative cross sections were determined to be slightly different, with Q^1 having the most different variation in cross section when compared with the other Q^n units. The greatest discrepancy between the present NMR results and the Raman data also occurs for the Q^1 unit, perhaps because of the oversimplifying assumption of equal Raman cross sections.

5. Conclusions

A ^{29}Si MAS NMR study was performed on lithium silicate glasses with lithium oxide contents as high as 64.3 mol%; this considerably extends the range of compositions studied by NMR. The results show deviations from the idealized lever rule reactions ($Q^n \rightarrow Q^{n-1}$) and considerable disproportionation takes place ($2Q^n \rightarrow Q^{n+1} + Q^{n-1}$). Volumes per mole silica show conjoined linear regions whose slopes increase in discrete steps as lithia content increases; this is seen resulting from the observed systematic changes in short-range order. The present NMR data are in substantial agreement with a Raman spectroscopic study of similar highly modified lithium silicate glasses.

Acknowledgments

The NSF of the USA is thanked under grants DMR 0211718 and DMR 05020518. The EPSRC of the UK is acknowledged for funding of the NMR facility at Warwick and for a Visiting Fellowship for Feller. Coe College is thanked for providing much student support including summer housing. The University of Warwick is appreciated for its hospitality to C Larson, J Doerr and S Feller during their stays there.

References

[1] Duer M J (ed) 2002 *Solid-State NMR Spectroscopy: Principles and Applications* (Oxford: Blackwell Science) pp 73–75 and 398–405

[2] Dupree R, Holland D and Mortuza M G 1990 A mass NMR investigation of lithium silicate glasses and glass ceramics *J. Non-Cryst. Solids* **116** 148–60

[3] Maekawa H, Maekawa T, Kawamura K and Yokokawa T 1991 The structural groups of alkali silicate glasses determined from ^{29}Si MAS-NMR *J. Non-Cryst. Solids* **127** 53–64
[4] Kasper J, Feller S and Sumcad G 1984 New sodium-borate glasses *J. Am. Ceram. Soc.* **67** C71
[5] Shelby J E 2005 *Introduction to Glass Science and Technology* 2nd edn (Cambridge: RSC) pp 82–90
[6] Dupree R, Ford N and Holland D 1987 An examination of the ^{29}Si environment in the PbO–SiO_2 system by magic angle spinning nuclear magnetic resonance. Part 1. Glasses *Phys. Chem. Glasses* **28** 78–84
[7] Peters A M, Alamgir F M, Messer S W, Feller S A and Loh K L 1994 The density of lithium silicate glasses over an extended range of compositions *Phys. Chem. Glasses* **35** 212–5
[8] Bansal N P and Doremus R H 1986 *Handbook of Glass Properties* (London: Academic) pp 54–55
[9] Umesaki N, Iwamoto N, Tatsumisago M and Minami T 1988 A structural study of rapidly quenched glasses in the system Li_2O–SiO_2 *J. Non-Cryst. Solids* **106** 77–80